

# The Study of Corrosion Behaviour of Cobalt-Iron (CoFe) Alloy Coating

Nor Fazli Adull Manan\*, Nik Rozlin Nik Mohd Masdek, Abdul Qayyum Abdul Aziz, Zuraidah Salleh

Faculty of Mechanical Engineering, Universiti Teknologi MARA, 40450 Shah Alam, Selangor, Malaysia

\* norfazli@salam.uitm.edu.my

## ABSTRACT

*Cobalt-Iron (CoFe) nanocrystalline alloy coating were successfully electrodeposited in a sulfate bath by supplying direct current to the 304-stainless steel and AISI 1080 mild steel substrates. The objective of this research is to study the corrosion behaviour of deposited CoFe coating on the substrates by the characterization test and the corrosion rate test. The electrodeposition method was done by controlling the operating parameter such as temperature, pH, current, deposition time and sulfate bath composition. The bath temperature was maintained at 40 °C for 30 minutes with an acidic condition of pH 3.5. The iron content was varied at 1.39 g, 2.76 g, and 5.56 g to study its influence on the physical properties such as size of nanoparticles, phase and crystallographic structure, surface roughness and microhardness of CoFe coatings. The CoFe nanocrystalline of 1018 mild steel with 2.76 g Fe content achieved the highest average microhardness of 324.32 HV compared to 304 stainless steel. The experimental result from X-Ray Diffraction (XRD) test shows that the particles sizes of CoFe alloy coating decreases with an increase of Fe content. Furthermore, it was found that the highest surface roughness recorded is 9.86 µm for 2.76 g of Fe content. Also, a potentiodynamic polarization test (PDP) method was used to assess the corrosion performance of the coating on each substrate material. At the end of the research, the corrosion*

*resistance of the CoFe alloy on 304 stainless steel substrate has better corrosion resistance than AISI 1018 mild steel.*

**Keywords:** *CoFe, nanocrystalline, potentiodynamic, electrodeposition, X-Ray Diffraction.*

## **Introduction**

A nanocrystalline material is a polycrystalline with a crystallite size of only a few nanometers. These materials fill the gap between amorphous materials without any long range order and conventional coarse-grained materials. Their definitions vary, but nanocrystalline materials are commonly defined as polycrystalline materials that contain an average grain size below 100 nm [1]. Nanocrystalline materials were found to have unique and improved properties in terms of their mechanical, chemical and physical properties compared to their conventional polycrystalline counterparts [2]. The electrodeposition technique is found to be the best and simpler method to generate nanocrystalline materials because of its straight-forward and low cost process, and the possibility of deposition is feasible on almost any geometry of a conductive substrate [3]. Various metallic coatings have been produced by the electrodeposition process such as (NiCo), (ZnCo), and (NiFe).

Nowadays, electrodeposited cobalt iron (CoFe) alloys are also gaining much attention in the wide application range of magnetic recording, electronics industries and protective coatings due to their high saturation of magnetic flux and high Curie temperature [4]. In this study, nanocrystalline of CoFe is synthesized by the electrodeposition method in a water bath while varying the iron concentration and other deposition parameters on stainless steel and mild steel substrates. The electrodeposition of both cobalt and iron simultaneously exhibit anomalous co-deposition which indicates that reduction of cobalt is inhibited while the deposition of iron is enhanced. The iron content of the deposits is not affected when applying various temperatures during the electrodeposition process although the surface morphology was seen to yield pits at high deposition temperature [2].

Several researchers have reported that the magnetic saturation of CoFe alloy had increased with an increase in iron content in the deposit. The homogeneous magnetic fields significantly affected the electrodeposited CoFe properties in terms of their microstructure, roughness, internal stress state, and chemical composition [5]. A study in terms of tensile stress reported that grain size plays an important role on the tensile stress of CoFe coatings where smaller the grain size leads to higher tensile stress of the electrodeposits and also decreasing of the grain size will reduce the penetration current density and result in uniform and better localized corrosion resistance due to highly distributed current [6]. Other than that, a study on the increase of iron content also resulted in an increase of stress in the alloy deposit. Although many researches have been done on coatings of CoFe alloys in terms of their magnetic properties and stress, only a few had been done on the development of nanocrystalline CoFe alloys. Therefore, in this work, the effects of varying iron content of the sulfate bath on the microstructure, crystallographic structure, grain size, surface roughness and microhardness on substrate materials will be investigated and finally conclude which substrate materials have the best corrosion resistance.

## **Methodology**

### **Electrodeposition of CoFe**

Electrodeposition method using standard two electrode cell configuration cell was used to synthesize the nanocrystalline CoFe coating. Figure 1 shows a 304 stainless steel substrate with dimensions 9 mm x 5 mm (exposed area is 268.61 mm<sup>2</sup>) and Figure 2 shows an AISI 1018 mild steel substrate with dimensions 8 mm x 5 mm (exposed area is 226.19 mm<sup>2</sup>) were used as a cathode substrates while a graphite rod was used as an anode substrate and was placed 2 cm from the cathode. The substrates were bonded to a copper wire using a conductive silver epoxy to establish an electrical connection. Before the electrodeposition process, the specimen was polished using emery papers of 400, 600 and 1200 grit sizes, followed by mirror polished using cloth polishing wheel machine and rinsed with distilled water. Then, the specimens were immersed in sulfuric acid for several

seconds to eliminate excess contaminants. Specimens were then weighed before and after the electrodeposition process.

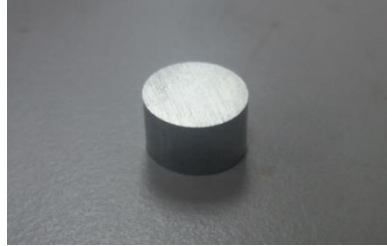


Figure 1. 304-stainless steel



Figure 2. AISI 1018 mild steel

The water bath for CoFe deposits consisted of cobalt sulfate ( $\text{CoSO}_4$ ), iron sulfate ( $\text{FeSO}_4$ ), sodium chloride ( $\text{NaCl}$ ), boric acid ( $\text{H}_3\text{BO}_3$ ) and saccharin ( $\text{C}_7\text{H}_4\text{NO}_3\text{S}$ ). Boric acid and saccharin were added as a pH buffer and grain refiner, respectively. Iron sulfate concentration was adjusted to produce CoFe deposits with various iron contents. The chemicals composition of the solution is shown in the Table 1.

Table 1. Bath composition for CoFe electrodeposition.

Variable	Range
$\text{CoSO}_4$ , (g)	7.0272
$\text{FeSO}_4$ , (g)	1.39, 2.76, 5.56
$\text{H}_3\text{BO}_3$ , (g)	8.244
$\text{NaCl}$ , (g)	2.0
Saccharin,(g)	0.6836

All chemicals were mixed in a beaker filled with 400 ml distilled water. By using a magnetic stirrer, the sulfate bath was constantly stirred in order to ensure the electrolyte was properly mixed in the solution while maintaining the temperature at 40°C and applied direct current maintained between the range of 0.7 A to 1.0 A. The pH bath was maintained at acidic state which is pH 3.5 and the deposition time was carried out for 30 minutes. Each of the experiments was carried out with freshly prepared sulfate bath to maintain its composition freshness. The specimens were ran with constant parameters except with variation of FeSO<sub>4</sub> content 1.39 g, 2.76 g and 5.56 g, respectively. Post plating, the deposits were immediately taken out from the solution and rinsed with distilled water to ensure unwanted salts on the surfaces were removed. The deposits were then dried straight away for a moment in room temperature. Figure 3 illustrates the schematic diagram of the electrodeposition process.

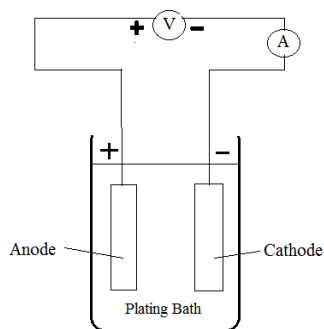


Figure 3. Schematic diagram of electrodeposition process.

## **Characterization**

The phase formation of CoFe nanoparticles was characterized using ULTIMA IV FD 3668N, X-Ray Diffraction (XRD) using Cu K $\alpha$  radiation (40 kV, 40 mA) at a scan rate of 5°/min. The XRD data were recorded in a range of 30° to 90°. XRD was used to identify the preferred crystallographic orientation as well as calculate grain sizes of the electrodeposits. The average grain size of crystallites was

calculated using the Scherrer formula according to the XRD peak broadening.

The Microhardness of CoFe nanoparticles was measured using a MITUTOYO MVK-H1, Vicker Microhardness tester with a pyramidal indenter under a load of 1kg for 15s. Five readings were taken at different locations about the alloy coating surface and the average value was taken as the final hardness value. The Infinite Focus Metrology (Alicona) machine was used to study the surface roughness of CoFe nanoparticles. Different spots on the coating surfaces were selected to obtain the average value of the surface roughness profile,  $R_a$ .

### **Corrosion Test**

A conventional three electrode cell was used which consisted graphite as the counter electrode, CoFe alloy coating as the working electrode and saturated calomel electrode (SCE) as the reference electrode. Potentiodynamic Polarization test (PDP) was conducted to evaluate the corrosion behaviour of nanoparticles using the GAMRY brand equipment. The potentiodynamic polarization test was performed in 0.1M NaOH (pH 8) solution. The open circuit potential (OCP) was carried out for 50 minutes to allow working electrodes to reach steady state conditions. The PDPs were performed with a scan rate of 0.5 mV/s.

## **Result And Discussion**

### **XRD Analysis**

All of the XRD patterns for CoFe nanoparticles were measured from  $2\theta$  angle of  $30^\circ$  to  $90^\circ$  using Cu  $K\alpha$  radiation at a scan rate  $5^\circ/\text{min}$ . X-Ray diffraction patterns of CoFe nanoparticles for 1018 Mild steel and 304 stainless steel at iron content 1.39 g, 2.76 g, and 5.56 g are shown in Figure 4 and Figure 5 below.

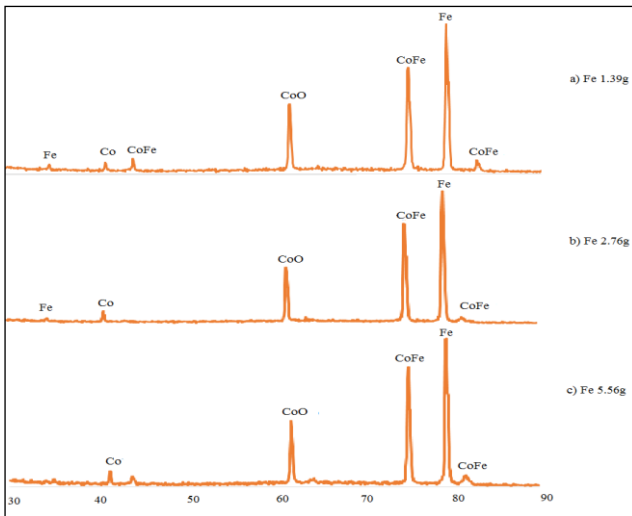


Figure 4. XRD patterns of CoFe alloy coatings for 1018 mild steel at various iron content

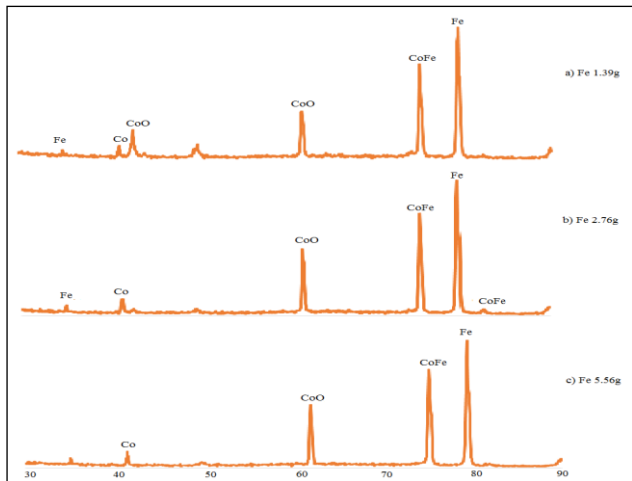


Figure 5. XRD patterns of CoFe alloy coatings for 304 stainless steel at various iron content

From the results, the XRD pattern shows that all samples consist of Co (Cobalt), CoO (Cobalt Oxide), Fe (Iron), CoFe (Cobalt iron) peak positions, nonetheless, the influence of the variation iron composition. All the results for the peak status was verified and matched with standard data from the standard XRD library data for CoFe compound. Each peak characteristic of CoFe is reflected with their crystallographic structure on the coating. All deposits were seen to have similar crystallographic structures at the same peak positions about  $74^\circ$  corresponding to CoFe (210) of the cubic structure. The Co (100) revealed its characteristic peaks at  $41.68^\circ$  for all samples and were recognized as Hexagonal Close Packed (HCP). The Fe (110) were seen at  $78^\circ$  and recognized as Body Centered Cubic (BCC). Deposits with 1.39 g and 2.76 g iron content exhibited Body Centered Cubic (BCC) and Face Centered Cubic (FCC) crystal structures.

As the iron content increased to 5.56 g, the deposits exhibited a BCC crystal structure phase only. The results obtained was accordance with previous study done [7] where crystal structures change with different range of iron content present in the coating. Moreover, research done by Afshari [8] demonstrates that higher iron amount in deposits increases the peak position and shifts to higher angles. Apart from that, we can observe that there another contaminant was present in the coating which is CoO (220) at  $61.80^\circ$  angle. As mentioned by Alfantzi [9], this compound existed due to the oxidation process when the samples was not properly cleaned to remove excess contaminants before coating process.

## Grain Size

The grain size of the CoFe alloy coating were measured from the line broadening of the X-ray peaks from XRD according to Scherrer's equation (1) which is as follows [10]:

$$D = \frac{k\lambda}{\beta \cos \theta} \quad (1)$$

where D is the average crystallite size,  $\lambda$  is the wavelength of the radiation,  $\theta$  is the Bragg angle and  $\beta$  is the full width half maximum (FWHM). All the grain size of the CoFe nanoparticles were observed

to be decrement with an increment of iron content of the coating as shown in Table 2 below. For 304 stainless steel, the highest average grain size value is 42.73 nm which is at 1.39 g and the lowest grain size value is 40.67 nm at 5.56 g. While for 1018 mild steel, it is shown that the coating with iron content 1.39 g recorded grain sizes of about 44.74 nm. Smaller grain sizes of 37.85 nm was achieved at the highest iron content 5.56 g. The results obtained are reported to be the same in studies concerning about the grain refining due to increase of iron content in the deposit [10,11].

Table 2. Crystalline Size of CoFe nanoparticles

Substrate	304 Stainless steel	1018 Mild Steel
Iron Content(g)	Crystallite Size (nm)	
1.39	42.73	44.74
2.76	41.72	38.07
5.56	40.67	37.85

### **Microhardness**

The microhardness of CoFe nanocoating was measured by using a Vickers MicroHardness tester with pyramidal indenter. A load of 1 kg was applied on the flat surface of CoFe coated substrate for an indentation time about 15 s. The final value of microhardness was taken with an average of 5 measurements taken from different locations on the surface of CoFe coatings. Figure 5 below shows the change of hardness properties with function variation of Fe content at 1.39g, 2,76g, and 5.56g on each substrate.

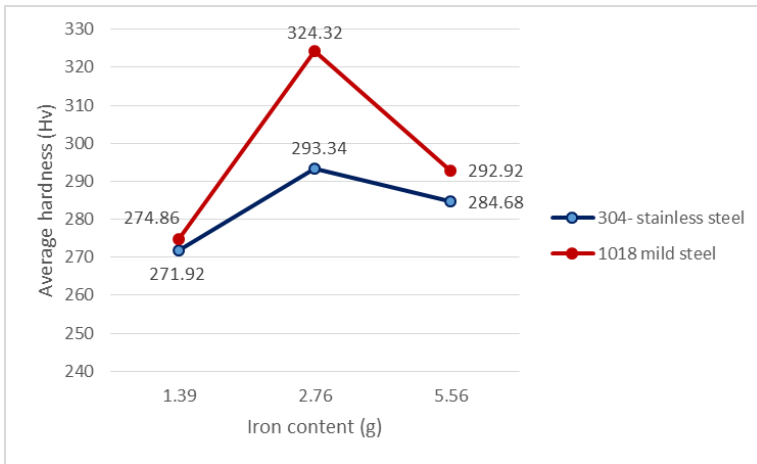


Figure 6. The average microhardness with variation of Fe content

Based on the Figure 6, 1018 mild steel shows a rapid increase in hardness for deposits with an Fe content of 1.39 g at 274.86 HV to 2.76 g at 324.32 HV, and then decreased at 292.92 HV for 5.56 g. While for 304 stainless steel, there is an increment of hardness from 271.92 HV to 293.34 HV, and then a slight decrease to 284.68 HV. The average hardness at 2.76 g Fe content was measured to be higher than at 1.39 g and 5.56 g Fe content for both substrates. The highest hardness for 1018 mild steel was measured at 324.32 HV which is the highest compared to 293.34 HV for 304 stainless steel. The steady increase obtained at lower Fe content and the decline at higher Fe content can be related to the change of phase structure and particle size of the nanocrystalline deposits. The smaller the particle size, the greater number of particle boundaries and high grain boundaries in the microstructure [12].

The existence of these grain boundaries cause increase of microhardness particles. In addition, research by Suryanarayana [13] reported that the decreasing of particle size resulted in the rise of hardness of nanocrystalline materials. Another factor effecting the changing behaviour of microhardness due to grain size is the rise at lower Fe content because of the refinement in grain size as the Fe content increases which is in conformance with the study by Li and Ebrahimi [14] about increasing hardness of NiFe. They reported that the solid solution hardening with an increase of Fe causes the strength to increase. Apart from that, the decreasing of hardness at higher Fe content was due to the solid solution hardening which is no longer

effective. According to T. Yamasaki [15], the significant increase of the intercrystalline volume fraction associated with fraction of triple junction caused the softening grain refinement of grain size.

## **Surface Roughness**

There are many different roughness parameters used, but Ra is by far the most common used for research. Figure 7 below shows the average value of surface roughness obtained for 304 stainless steel and 1018 mild steel. Based on the results, the average value of surface roughness was measured to be varied according to the iron composition of all the coating samples. Both of the samples show an increment of surface roughness at the initial lower iron content and then decreasing at higher iron content. The highest average value of surface roughness recorded is for the coating sample with the iron composition of 2.76 g at 9.842  $\mu\text{m}$  for 1018 mild steel and 8.694  $\mu\text{m}$  for 304 stainless steel. Meanwhile, the lowest average value of surface roughness recorded came from the coating's iron composition 1.39 g is at 2.602  $\mu\text{m}$  for 304 stainless steel and 4.287  $\mu\text{m}$  for 1018 mild steel.

The maximum average value of the surface roughness recorded for the iron composition 2.76 g, is due to the presence of voids that has been reported by previous research [12]. The formation of voids occur due to the oxidation process which happened when the CoFe coating was not properly stored in a vacuum surrounding [16]. In addition, as mention by Koay [17], the voids are present when there is hydrogen evolution at the electrode surface during the electrodeposition process. Besides that, the decrement of average value of surface roughness is because the formation of initial cluster that have smaller particle size and dense population which happened to be due to the rise of nucleation density [18]. When surface diffusion of adatoms on the coating surface was unimpeded, it is expected that there is formation of large nuclei.

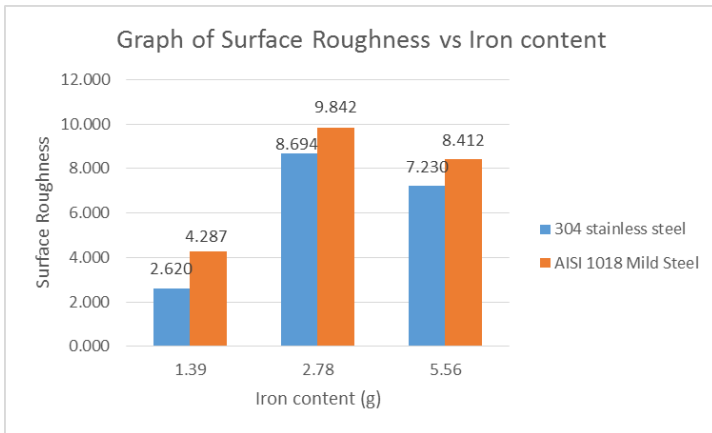


Figure 7. Graph of Average surface roughness (Ra) vs Iron Content (g)

### Potentiodynamic Polarization

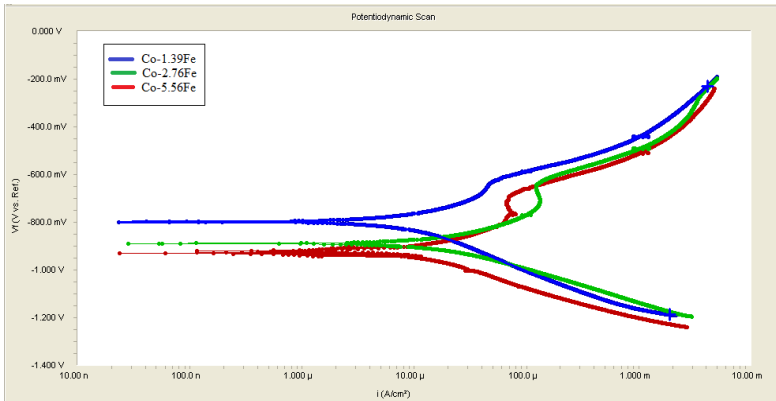


Figure 8. Potentiodynamic polarization curves of CoFe on 304 SS with various iron content

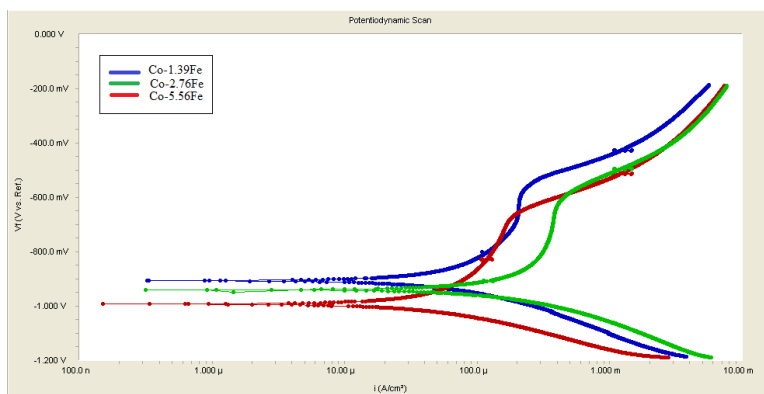


Figure 9. Potentiodynamic polarization curves of CoFe on 1018 S with various iron content

The polarization test for CoFe coating were carried out on both 304 SS and 1018 MS in alkaline medium. The scan started from cathodic potential region and was further continue to anodic region. Figure 8 and 9 shows typical polarization curves obtained from nanocrystalline CoFe deposits on 304 SS and 1018 MS. It can be observed that the polarization curves of all samples have a generally similar behaviour that contain typical active-passive-transpassive behaviour. The passivation stage starts at an electrode potential of -900mV for both substrate materials. The formed passivation film reported to consist of  $\text{Co(OH)}_4$  that exhibit effect on the passivation behaviour. Similar corrosion behaviour for CoFe coatings was also reported from previous studies [6] that stated that passivation stages at the same range due to being controlled by the presence of porous film of  $\text{Co(OH)}_4$ .

Table 3 summarizes the potentiodynamic results. It can be seen that with an increase in iron content, the corrosion potential ( $E_{\text{corr}}$ ) move to a more negative potential from -798 mV to -929 mV for 304 SS and -906 mV to -992 mV for 1018 MS. Besides that, the current density shows a decrement with an increase in iron content from  $7.83 \mu\text{A}/\text{cm}^2$  to  $4.20 \mu\text{A}/\text{cm}^2$  for 304 SS and from  $48.60 \mu\text{A}/\text{cm}^2$  to  $44.10 \mu\text{A}/\text{cm}^2$  for 1018 MS. This shows that an increase in iron content will reduce the grain size and will influence on the passive behaviour of nanocrystalline CoFe coatings. There have been reports of similar observations of improved corrosion behaviour for nanocrystalline materials in alkaline medium [8,16]. This happened due to the high density of nucleation sites presents in CoFe coatings which caused rapid formation of protective passive layer. This stable protective

passive layer blocks the ions or electrons from moving toward the surface to participate in the electrochemical reaction.

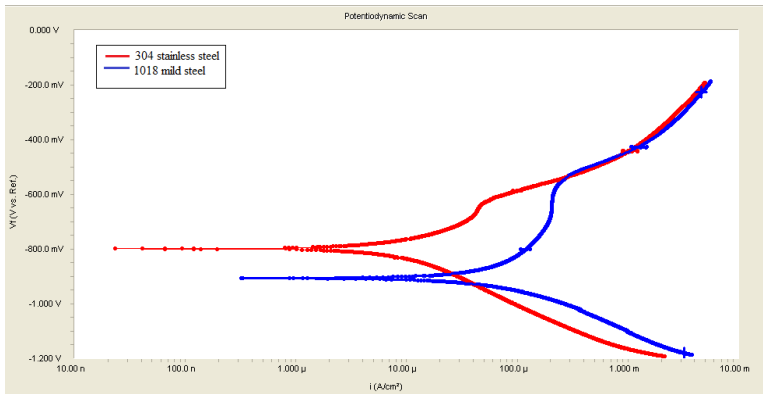


Figure 10. Potentiodynamic polarization curves of CoFe (1.39g) on 304 stainless steel and 1018 mild steel

Table 3. Potentiodynamic polarization data of CoFe alloy coating in 0.1M NaOH

Substrate material	304 Stainless steel			1018 Mild steel		
	Corrosion rate (mmpy)	E <sub>corr</sub> (mV)	I <sub>corr</sub> (μA/cm <sup>2</sup> )	Corrosion rate (mmpy)	E <sub>corr</sub> (mV)	I <sub>corr</sub> (μA/cm <sup>2</sup> )
CoFe(1.39g)	7.814	-798.00	7.83	32.840	-906.00	48.60
CoFe(2.76g)	4.993	-889.00	5.00	38.500	-940.00	45.20
CoFe(5.56g)	17.170	-929.00	4.20	46.940	-992.00	44.10

The corrosion performance of CoFe coatings on both substrate was assessed in 0.1M NaOH of 250 ml electrolyte with an alkaline condition maintained at pH 8±9 through the testing process. The corrosion rate is recorded as shown in Table 3. From Table 3, we can see that the electrolyte with lower iron concentration to be least corrosive. Higher iron concentration shows bigger corrosion rates for respective materials. Generally, both substrates show an increase of corrosion rate as the iron concentration in CoFe coating increases. It can be observed that, the highest corrosion rate of 304 stainless steel at 17.170 mmpy is still lower than the lowest corrosion rate of 1018 mild steel at 46.940 mmpy. Figure 10 illustrates that there are differences between Tafel’s slopes for different substrates. These differences may be attributed to the nature of each substrate surface or to changes in the electrode potentials of each substrate. The 304 SS substrate reveals

enhanced corrosion performance, with the noblest (less negative) corrosion potential  $-798\text{mV}$  compared to 1018 MS corrosion potential  $-906\text{mV}$ . Higher corrosion potential result in better corrosion performance [19]. In addition, increase in corrosion resistance of deposits on 304 SS substrate due to the noble nature of 304 SS which resulted in little interaction with its surface and the alloy components [20]. This shows that deposited CoFe on 304 stainless steel substrate have better corrosion resistance than the 1018 mild steel substrate. A previous research [21] had also shown the same result where corrosion resistance of deposited on 304 stainless steel substrate was better than of mild steel.

## **Conclusion**

CoFe nanoparticles with various iron concentration was successfully synthesized on 304 SS and 1018 MS by electrodeposition process. From this study, it was discovered that the increase of Fe content has a major influence on the crystallite size, average microhardness, surface roughness, and corrosion behaviour of the CoFe nanoparticles. The crystallite size was recorded between the range of  $37.85\text{ nm}$  to  $44.74\text{ nm}$  for 1018 MS and  $40.67\text{ nm}$  to  $42.73\text{ nm}$  for 304 SS. Other than that, the grain size were found to be smaller with the increase of iron content. Furthermore, the average microhardness of the CoFe nanoparticles were also affected by the iron content. The CoFe nanoparticles at  $2.76\text{ g}$  iron content on 1018 MS achieved highest average microhardness  $324.32\text{ HV}$  compared to 304 SS. From this study, it can be deduced that CoFe coating on 304 SS substrate at  $1.39\text{ g}$  iron content has the smoothest coating surface compared to others. On the other hand, the corrosion rate of CoFe nanoparticles accelerated with the increment of iron content. The CoFe coating on 304 SS substrate shows a better corrosion resistance compared to the CoFe coating on 1018 MS even though the higher corrosion potential of 304 SS substrate influences the corrosion performance.

## **Acknowledgment**

This research was sponsored by Universiti Teknologi MARA (UiTM) Malaysia, grant no. (UiTM File. No. 600-RMI/DANA 5/3/LESTARI (67/2015)). The analyses was conducted at Faculty of Mechanical Engineering, Universiti Teknologi MARA, 40450 Shah Alam,

## References

- [1] H. Gleiter, *Materials With Ultra-Fine Grain Sizes, Proceedings of the 2nd Riso International Symposium on Metallurgy and Materials Science*. Roskilde, 1981.
- [2] N. M. Nik Rozlin and A. M. Alfantazi, "Nanocrystalline cobalt-iron alloy: Synthesis and characterization," *Mater. Sci. Eng. A*, vol. 550, pp. 388–394, 2012.
- [3] F. Lallemand, L. Ricq, E. Deschaseaux, L. De Vettor, and P. Ber??ot, "Electrodeposition of cobalt-iron alloys in pulsed current from electrolytes containing organic additives," *Surf. Coatings Technol.*, vol. 197, no. 1, pp. 10–17, 2005.
- [4] E. E. Kalu, "Properties of nanocrystalline electrodeposited CoFeP alloy with low phosphorus content," *J. Solid State Electrochem.*, vol. 11, no. 9, pp. 1145–1156, 2007.
- [5] J. George, S. Elhalawaty, A. J. Mardinly, R. W. Carpenter, D. Litvinov, and S. R. Brankovic, "Electrochimica Acta Oxide / hydroxide incorporation into electrodeposited CoFe alloys — Consequences for magnetic softness," *Electrochim. Acta*, vol. 110, pp. 411–417, 2013.
- [6] K. H. Kim, S. H. Lee, N. D. Nam, and J. G. Kim, "Effect of cobalt on the corrosion resistance of low alloy steel in sulfuric acid solution," *Corros. Sci.*, vol. 53, no. 11, pp. 3576–3587, 2011.
- [7] H. Abdel-Karim, R., Reda, Y., Muhammed, M., El-Raghy, S., Shoeib, M., and Ahmed, "Electrodeposition and Characterization of Nanocrystalline Ni-Fe Alloys," *J. Nanomater.*, vol. volume 201, no. 7, 2011.
- [8] C. Afshari, V., Dehghanian, *Effects of grain size on the electrochemical corrosion behaviour of electrodeposited nanocrystalline Fe coatings in alkaline solution*, Vol. 51,ed. Corrosion Science, 2009.
- [9] A. Aledresse and A. Alfantazi, "A study on the corrosion behavior of nanostructured electrodeposited cobalt," *J. Mater. Sci.*, vol. 39, no. 4, pp. 1523–1526, 2004.
- [10] A. Monshi, M. R. Foroughi, and M. R. Monshi, "Modified Scherrer Equation to Estimate More Accurately Nano-Crystallite Size Using XRD," vol. 2012, no. September, pp. 154–160, 2012.
- [11] N. M. Nik Rozlin and A. M. Alfantazi, "Electrochemical properties of electrodeposited nanocrystalline cobalt and cobalt-iron alloys in acidic and alkaline solutions," *J. Appl. Electrochem.*, vol. 43, no. 7, pp. 721–734, 2013.
- [12] N. Azrina Resali, K. Mei Hyie, M. N. Berhan, Z. Salleh, and S.

- Kasolang, "Cobalt-Nickel-Iron Nanoparticles Coated on Stainless Steel Substrate," *Procedia Eng.*, vol. 68, pp. 30–36, 2013.
- [13] C. Suryanarayana, "The Structure and Properties of Nanocrystalline Materials : Issues and Concerns," pp. 24–27.
- [14] F. Ebrahimi and D. M. R. Award, "Deformation and Fracture of Nanocrystalline Metals Deformation and Fracture of Nanocrystalline Metals," 2000.
- [15] T. Yamasaki, "High-Strength Nanocrystalline Ni-W Alloys Produced by Electrodeposition," vol. 1, no. 2000, pp. 127–132, 2010.
- [16] M. J. G. and F. A, "MYTRIBOS," in *Proceedings of Malaysian International Tribology Conference*, 2015, p. 33.
- [17] K. Mei, N. Azrina, W. Normimi, R. Abdullah, and W. T. Chong, "Synthesis and Characterization of Nanocrystalline Pure Cobalt Coating : Effect of pH," vol. 41, no. Iris, pp. 1627–1633, 2012.
- [18] S. H. LeeM. G. So, "Effects of deposition temperature and pressure of the surface roughness and the grain size of polycrystalline Si<sub>1-x</sub>Gex films," *J. Mater. Sci.*, vol. 35, no. 19, pp. 4789–4794, 2000.
- [19] J. Chen, R. M. Asmussen, D. Zagidulin, J. J. Noël, and D. W. Shoesmith, "Electrochemical and corrosion behavior of a 304 stainless-steel-based metal alloy wastefrom in dilute aqueous environments," *Corros. Sci.*, vol. 66, pp. 142–152, 2013.
- [20] M. M. Abou-Krisha, A. G. Alshammari, F. H. Assaf, and F. A. El-Sheref, "Electrochemical behavior of Zn-Co-Fe alloy electrodeposited from a sulfate bath on a various substrate materials," *Arab. J. Chem.*, pp. 0–7, 2015.
- [21] A. K. Singh, V. Chaudhary, and A. Sharma, "Electrochemical Studies of Stainless Steel Corrosion in Peroxide Solutions," vol. 30, no. 2, pp. 99–109, 2012.